

Thermal-energy collisions of rubidium Rydberg states with N₂ molecules

L. Petitjean, F. Gounand, and P. R. Fournier

Centre d'Etudes Nucléaires de Saclay, Service de Physique des Atomes et des Surfaces, Institut de Recherche Fondamentale, Commissariat à l'Energie Atomique, F-91191 Gif-sur-Yvette Cédex, France

(Received 17 February 1984)

The total depopulation cross sections by N₂ of high rubidium Rydberg states, Rb(*ns*) (*n* = 25–46) and Rb(*nd*) (*n* = 23–44), have been measured using time-resolved field ionization technique and compared to previous results obtained on the quenching of Rb(*nl*) by CO. It is shown that the Rb(*nl*) depopulation by N₂ is much less efficient than the Rb(*nl*) depopulation by CO and leads mainly to the quasielastic process of angular momentum mixing via the short-range interaction between the quasifree Rydberg-state electron and the molecule. It is clearly demonstrated that the presence of a permanent dipole in CO changes the collisional processes drastically. The agreement between experimental and theoretical predictions based on the impulse approximation is quite satisfactory.

I. INTRODUCTION

Previously, we studied the quenching cross sections of highly excited *s* and *d* states of Rb by CO molecules.¹ The conclusions of this previous paper (to be referred to as paper I hereafter) can be summarized as follows. The total depopulation cross section is expressed as a sum of the following three terms:

$$Q = \sigma_{l \text{ mixing}} + \sigma_{n \text{ changing}} + \sigma_{\text{ionization}}, \quad (1)$$

where the *l* mixing² is produced by the short-range interaction between the quasifree Rydberg electron and the molecule, *n* changing and ionization being due to the long-range *e*⁻-molecular-dipole interaction (the *e*⁻-quadrupole interaction has been found to be less efficient than the *e*⁻-dipole interaction even for a weak dipole like CO). The *e*⁻-dipole interaction leads to quiresonant energy transfer where the internal energy (atomic or rotational) lost by one colliding partner is gained by the other. We have found in the studied range of *n* (= 23–45) that this rotational energy transfer is generally dominant over the quasielastic process of *l* mixing. For *s* and *d* states,³ the calculated *l*-mixing cross section is about one order of magnitude lower than the quenching cross section by CO.

For a homonuclear molecule like N₂ the quenching cross section when neglecting the quadrupole moment should be equal to the *l*-mixing cross section which is given in the impulse approximation⁴ by

$$\sigma_{l \text{ mixing}} = \frac{2\pi L^2}{V^2} \int_{|k-k'|}^{k+k'} F_{nl, n'l'}(K) K dK \quad (2)$$

with *L* the *e*⁻-perturber elastic scattering length, *V* the relative velocity of the Rydberg atom-perturber system, *k* and *k'* the wave vectors of the relative motion before and after collision, *K* the momentum transferred in the collision, and *F*_{*nl, n'l'*}(*K*) the squared atomic transition form factor [atomic units (*m_e* = *e* = \hbar = 1) are used unless otherwise stated]. When comparing N₂ and CO molecules we may say that, crudely speaking, these two molecules only differ by the existence of the CO dipole. Since N₂ and CO

have equal masses, the kinematics of the collision is the same for the two molecules and it is easy to see that we have

$$\sigma_{l \text{ mixing Rb}(nl)+N_2} = \left(\frac{L_{e-N_2}}{L_{e-CO}} \right)^2 \sigma_{l \text{ mixing Rb}(nl)+CO}. \quad (3)$$

In the range of electron energy of interest here we have (*L*_{*e-N*₂}/*L*_{*e-CO*})² ~ 0.5. Then the quenching cross section of high Rydberg states Rb(*nl*) by N₂, approximately given by the *l*-mixing term, should stay about one order of magnitude lower than the corresponding quenching cross section by CO. Thus we have the possibility to check experimentally the importance of the *e*⁻-dipole interaction in the total depopulation of a high Rydberg level by a polar molecule.

On the other hand some measurements on the depopulation of low lying (*n* ≤ 10) and intermediate (*n* ~ 10–20) Rydberg states by nitrogen molecules are available. The collisional depopulation of Na(*nd*) states from *n* = 5 to 14 by N₂ and CO has been studied by time-resolved laser fluorescence by Gallagher *et al.*⁵ For both CO and N₂ the cross sections rise sharply from *n* = 5 to 10 and remain constant for *n* > 10, while the quenching cross sections by N₂ and CO are comparable. In these collisions, *l* mixing provides the dominant depopulation mechanism and cross sections are comparable to those obtained for helium.^{6,7} This is not in contradiction with the predicted role of *e*⁻-dipole interaction because to be efficient such a process has to lead to energy-transfer reaction whose energy defect δ is small^{8,9} ($\delta < 2 \text{ cm}^{-1}$). For instance the energy separation between the Na (14*d*) and the *n* = 15 manifold is ~ 73 cm⁻¹, while the energy gained by the rotational transition *J* → *J* - 1 is 2*B*₀*J* (*B*₀ ~ 2 cm⁻¹); thus the lowest rotational level of CO that can contribute to *n* changing is *J* = 18 whose population in a cell experiment is quite low (~ 1%). Consequently due to the wide energy spacing between low-lying states only some transitions between high rotational levels may produce *n*-changing reactions and their relative importance in the total depopulation remains quite negligible for the Na(*nd*) states that

are rapidly mixed with the higher l states.

On the contrary the nonhydrogenic levels $\text{Na}(ns)$ and helium Rydberg ns states and the n -manifold states of Na and He exhibit a quite different behavior. The cross sections for deactivation of the Na $5s-9s$ and $n=5-8$ manifold states by N_2 are very much higher^{10,11} than those for He (Ref. 12) clearly stating the importance of the energetically accessible rotational and vibrational levels in N_2 . Nevertheless the quenching cross sections remain one order of magnitude lower than those for the corresponding nd levels.⁵ The experimental data of Czajkowski *et al.*¹³ on the $\text{Na}(ns)-\text{N}_2$ quenching cross section and those of Hitachi *et al.*¹⁴ concerning the collisional depopulation of helium Rydberg ns and n -manifold states by N_2 ($n < 9$) are of the same order of magnitude as those observed by Humphrey *et al.*¹¹ or those deduced using the model of Bauer *et al.*¹⁵ characterized by multiple potential-energy curve crossings from the initial to the final states through an intermediate ionic state.

Let us finally quote the work of Kachru *et al.*¹⁶ who have measured the N_2 - and CO -induced collisional broadening of forbidden ground-to-Rydberg state transitions in sodium using a trilevel echo technique. These measurements on $3s-ns$ (nd) broadening cross sections, n ranging from 4 to 41, differ in some respects from those observed with noble-gas perturbers. Nonetheless it appears quite difficult to establish a firm theoretical connection between the inelastic cross sections for the total depopulation and the broadening by the molecular target of spectral lines involving Rydberg levels.

If one excepts the work of Kachru *et al.*, all the previously mentioned studies deal with low-lying or intermediate excited states. In contrast, due to the close energy spacing of the high Rydberg states, the present study on $\text{Rb}(nl)-\text{N}_2$ collisions will allow us to compare the efficiency of the short-range interaction responsible for the quenching of $\text{Rb}(nl)$ by N_2 relatively to the short-range plus long-range interaction responsible of the $\text{Rb}(nl)$ depopulation by CO .

II. EXPERIMENT AND RESULTS

The experimental method has been described in detail in Ref. 17 so we shall only outline it here. The $\text{Rb}(nl)$ state $n=23$ to 45 and $l=0, 2$ is selectively populated by a two-pulsed laser excitation via the $5P_{3/2}$ level in a field-free cell at room temperature ($T \sim 293$ K) where a N_2 gas

TABLE I. Experimental results for the quenching cross sections of the $\text{Rb}(ns)$ and $\text{Rb}(nd)$ levels by N_2 .

Level	Q (\AA^2)	Level	Q (\AA^2)
25s	220±45	23d	100±25
28s	265±50	26d	175±35
31s	305±30	29d	200±30
34s	230±55	32d	175±30
37s	180±45	35d	130±25
40s	190±48	38d	165±35
43s	185±20	41d	120±30
46s	170±25	44d	140±30

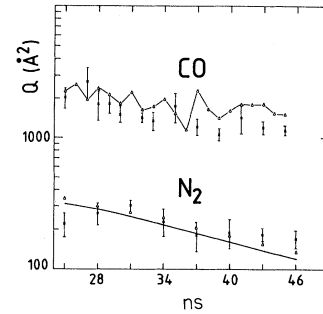


FIG. 1. Quenching cross sections for the $\text{Rb}(ns)$ levels by N_2 and CO versus the principal quantum number n . Experiment: $\frac{1}{\tau}$. The full curve represents the calculated l -mixing cross sections by N_2 when l mixing by CO —not shown in the figure—is a factor of 2 larger. The triangle (Δ) represents the total calculated cross section including l mixing, n changing and ionization. The line joining the triangle (Δ) is drawn for sake of clarity. All the CO values come from Ref. 1.

flow is maintained. The rubidium vapor pressure is about 2×10^{-7} Torr the nitrogen pressure varying from 0.1 to 5 mTorr. After a selected time delay within the range $0.4-10 \mu\text{s}$, during which collisions occur, the remaining nl states are field ionized. By measuring the effective life time τ of the nl state as a function of N_2 density n_{N_2} using a time-resolved selective field ionization technique we are able to determine the total depopulation cross section $Q(nl)$ via the well-known equation

$$\frac{1}{\tau} = \frac{1}{\tau_0} + n_{\text{N}_2} V_{\text{Rb-N}_2} Q(nl), \quad (4)$$

where τ_0 is the lifetime in the absence of collisions with N_2 , and $V_{\text{Rb-N}_2}$ the Maxwellian averaged relative velocity for Rb-N_2 collisions.

The experimental data are tabulated in Table I. They are compared to the quenching cross sections by CO (measured in I) in Fig. 1 for the ns levels and in Fig. 2 for

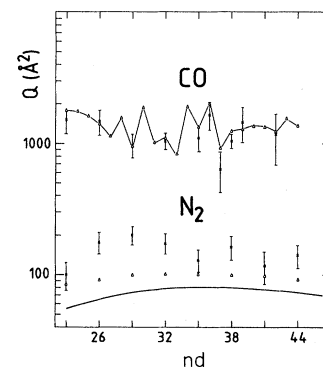


FIG. 2. Quenching cross sections for the $\text{Rb}(nd)$ levels by N_2 and CO versus the principal quantum number n . Experiment: $\frac{1}{\tau}$. The full curve represents the calculated l -mixing cross sections by N_2 when l mixing by CO —not shown in the figure—is a factor of 2 larger. The triangle (Δ) represents the total calculated cross section including l mixing, n changing and ionization. The line joining the triangle (Δ) is drawn for sake of clarity. All the CO values come from Ref. 1.

the nd levels. These figures clearly exhibit the difference between N_2 and CO ; the quenching cross section of high Rydberg states ($n > 23$) by N_2 is about one order of magnitude lower than for CO , as expected from the considerations developed in the Introduction.

III. THEORETICAL INTERPRETATION

We will use the same approach as in I to calculate the total depopulation cross section. According to the free-electron model the interaction potential in $Rb(nl)-N_2$ collisions is given by the e^-N_2 potential and expanded as

$$V = V_{e^-N_2 \text{ short range}} + V_{e^-N_2 \text{ long range}} \quad (5)$$

where the first term leads to the quasielastic processes of l mixing and the second one contributes to the inelastic transitions: n changing and ionization. The cross section for the transition $nl \rightarrow n'l'$ has been derived by Matsuzawa^{4,18,19} in the "impulse approximation" and is given by

$$\sigma_{nl, J \rightarrow n'l', J'} = \frac{2\pi}{V^2} \int_{|k-k'|}^{k+k'} |f_e(K)|^2 F_{nl, n'l'}(K) K dK, \quad (6)$$

where $|f_e|^2$ represents the squared scattering amplitude for the e^-N_2 collisions, i.e.,

$$e^- + N_2(J) \rightarrow e^- + N_2(J'), \quad (7)$$

where J and J' are the quantum numbers that specify the N_2 rotational quantum states.

Since the depopulation of the high Rydberg states will populate predominantly hydrogenic states $n'l' > 3$ (with $n' > 20$) whose energy are l' independent we are mainly interested in the sum over l' of the squared transition form factor $F_{nl, n'l'}$. We have recently shown²⁰ that the expression derived from the binary-encounter theory (BET) gives results in very good agreement with the quantal expression as far as the momentum transferred remains small and $n, n' \gg 1$. More precisely the BET expression of the total form factor is

$$F_{nl, n'}(K) = \frac{1}{2n'^3 K} \int_{|p_0|}^{\infty} |g_{nl}(p)|^2 p dp, \quad (8)$$

where $g_{nl}(p)$ is the radial wave functions in the momentum space and

$$p_0 = \left[-\frac{1}{2n'^2} + \frac{1}{2n^{*2}} - \frac{K^2}{2} \right] / K.$$

Explicit expressions of $F_{nl, n'}(K)$ were derived by Gounand and Petitjean.²⁰

For l -mixing collisions we have (Ref. 19) $|f_e|^2 = L^2$ with L the elastic scattering length given by the following:

$$4\pi L^2 = \sigma_{el}(1/2n^{*2}) \quad (9)$$

with σ_{el} the elastic scattering cross section at the electron energy $1/2n^{*2}$. σ_{el} has been averaged by de Prunelé and Pascale²¹ over the quantum-mechanical velocity distribution of the Rydberg electron and may be fitted in the energy range of interest by the following:

$$\sigma_{el} = 4.93 + \frac{77.3}{n^*} \quad (10)$$

with σ_{el} in atomic units.

The calculated l -mixing cross sections are reported in Table II for the ns levels and in Table III for the nd levels. They are also plotted (continuous line) in Figs. 1 and 2.

The long-range interactions between the Rydberg electron and N_2 is approximated by the first term in the potential multipole expansion

$$V(\vec{r}) = - \left[\frac{Q}{r^3} + \frac{\alpha'}{2r^4} \right] P_2(\hat{r} \cdot \hat{s}), \quad (11)$$

where r is the distance of the scattered electron from the center of mass of the molecule, s the internuclear distance and \hat{r}, \hat{s} the unit vectors. α' represents the nonspherical part of the polarizability, Q is the N_2 quadrupole and P_2 is the Legendre polynomial. The presence of P_2 selects inelastic rotational transitions with $\Delta J = \pm 2$ (this term also provides $J \rightarrow J \neq 0$ elastic transitions whose contribution to the l -mixing process is negligible). To calculate

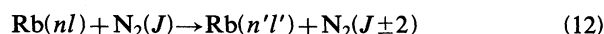
TABLE II. The first five columns give the depopulation cross sections for ns states via different processes. l mixing is produced by the short-range interaction between the Rydberg electron and N_2 when the e^-N_2 quadrupole long-range interaction is responsible for n changing and ionization. J_0 represents the lowest rotational level which contributes to the Rydberg ionization. The total depopulation of the Rydberg level is plotted in the last column. All the values are in \AA^2 .

$(n+3)s$	l mixing		n changing		Ionization (J_0)	Total depopulation
	$\rightarrow n$	$\rightarrow n-1$	Rydberg excitation	Rydberg deexcitation		
25s	308	4	18	13	0.005 (30)	343
28s	279	5	15	7	0.2 (23)	306
31s	244	6	17	8	0.8 (19)	276
34s	209	8	15	7	3 (15)	242
37s	178	9	12	6	4 (13)	209
40s	150	10	9	5	6 (11)	180
43s	127	12	8	4	8 (10)	159
46s	108	12	5	3	9 (9)	137

TABLE III. As in Table II but for nd states. All the values are in \AA^2 .

$(n+1)d$	l mixing		n changing		Ionization (J_0)	Total depopulation
	$\rightarrow n$	$\rightarrow n-1$	Rydberg excitation	Rydberg deexcitation		
23d	47	9	20	9	0.003 (30)	85
26d	55	11	16	10	0.1 (24)	92
29d	60	14	18	7	0.8 (19)	100
32d	62	16	15	6	2 (16)	101
35d	62	18	12	5	4 (13)	101
38d	60	20	9	4	6 (11)	99
41d	57	21	8	5	8 (10)	99
44d	53	21	6	3	9 (9)	92

the cross section of the quadrupole induced n changing



we have used for the scattering amplitude in Eq. (6) the first Born e^- -point quadrupole scattering amplitude, correct in the low-energy limit,^{22,23} following the work of Dalgarno and Moffett²⁴ which has shown that for e^- - N_2 low-energy collisions (< 0.1 eV) the polarization term α' in Eq. (11) may be neglected. The scattering amplitude is then given by the following:

$$|f_e(J \rightarrow J \pm 2)|^2 = \frac{2Q^2}{15} \frac{J_>(J_>-1)}{(J+J_>+1)(J+J_>-1)}, \quad (13)$$

where $J_>$ is the maximum of J and $J \pm 2$. Note that this expression is very similar to the scattering amplitude used for the l -mixing process; both are K independent.

The wave vector of the relative motion after the collision is given by the following energy conservation relation:

$$\frac{k^2}{2\mu} - \frac{1}{2n^*2} + E_J = \frac{k'^2}{2\mu} - \frac{1}{2n'^2} + E_{J \pm 2}, \quad (14)$$

where E_J represents the eigenenergy of the rotational state. The molecular data used are listed in Table IV and N_2 rotational distribution is plotted in Fig. 3.

Table V reports the cross section for process (12) with the $25s$ level. The resonant nature of the energy-transfer reaction may be demonstrated by the dependence of the cross section on the absolute values of the energy defect δ of the involved reaction. We have found it convenient to fit all the calculated cross section by a scaling law which holds for the ns and the nd levels ($23 < n < 46$) and reproduces the calculated cross section with an accuracy better than a factor of 3

TABLE IV. Molecular parameters of $\text{N}_2(X^1\Sigma_g^+)$ used in the calculations.

Rotational constant	B_e (cm^{-1})	1.998 24 ^a
	α_e (cm^{-1})	0.017 138 ^a
	D_0 (cm^{-1})	5.76×10^{-6} ^a
Quadrupole moment	Q (a.u.)	-1.1 ^b

^aReference 29.

^bReference 30.

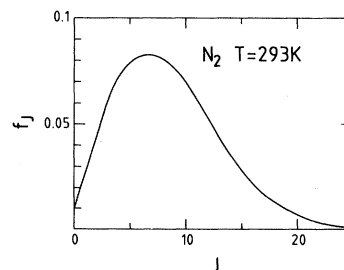
$$\sigma_{\text{scaling law}} = \frac{J_>(J_>-1)}{(J+J_>+1)(J+J_>-1)} \frac{1}{n_>^2 n^2} f(|\delta|), \quad (15)$$

where $n_>$ is the maximum of n, n' . The "resonance function" $f(x)$ is given by

$$f(x) = 7.2 \times 10^7 e^{-0.9x} (1 + 1.76x - 0.87x^2 + 0.113x^3), \quad (16)$$

where f and $x = |\delta|$ are, respectively, in \AA^2 and cm^{-1} .

In order to point out the quasiresonant nature of the internal energy transfer we have plotted the normalized resonance function for N_2 and CO (Ref. 23, paper I) versus $|\delta|$ in Fig. 4. Despite the accuracy of both scaling laws the comparison between the two cases allows to conclude that the dipole induced energy transfers have more pronounced resonant nature than the quadrupole induced energy transfers. This is clearly due to the longer range of the dipole interaction. The K dependence of the scattering amplitude is fixed by an integration over r ,²⁵ the distance of the electron from the center of mass of the molecule. The e^- -quadrupole potential falls off as r^{-3} leading to a K -independent scattering amplitude [Eq. (13)], while the e^- -dipole potential falls off as r^{-2} yielding a scattering amplitude proportional to K^{-1} . The integral in Eq. (6) is sharply peaked in the vicinity of the lower limit value²⁰ (related to the energy defect of the reaction). Thus for small momentum transfer, the integrand is much more sensitive to the energy defect in the

FIG. 3. Rotational distribution f_J versus rotational quantum number J for the N_2 molecule at $T=293$ K:

$$f_J = \frac{(2J+1)e^{-B_0 J(J+1)/kT}}{\sum_{J=0}^{\infty} (2J+1)e^{-B_0 J(J+1)/kT}}$$

TABLE V. Calculated cross sections σ for transitions: $25s + N_2(J) \rightarrow n' + N_2(J \pm 2)$. δ represents the energy defect of the transition. The scaling law is given by Eqs. (15) and (16). f_J represents the rotational distribution of the J level. The transition cross section has been computed up to $J=20$ for $\Delta J = -2$ and the sum of $\sigma_{n,J \rightarrow n', J-2} f_J$ over J reaches 18 \AA^2 . $\Delta J = 2$ transitions have been computed up to $J=30$ and the sum is 13 \AA^2 .

	J	Final hydrogenic state	δ (cm^{-1})	σ (\AA^2)	σ scaling law	σf_J
$J \rightarrow J-2$	3	23	-2.13	16.8	13.4	1.0
	4	23	5.83	3.1	1.2	0.2
	5	24	-3.14	10.3	4.5	0.8
	6	24	4.81	4.7	1.4	0.4
	7	25	-2.17	18.6	13.7	1.6
	8	25	5.78	3.0	1.1	0.2
	9	26	0.48	58.1	52.8	4.5
	10	27	-3.37	8.0	3.1	0.6
	11	27	4.57	4.3	3.1	0.3
	11	28	-5.99	2.1	3.1	0.1
	12	28	1.96	20.5	14.7	1.1
	13	29	0.41	43.7	44.7	1.9
	14	30	-0.21	39.8	42.4	1.4
	15	31	-0.02	36.2	36.8	1.0
	⋮					
$J \rightarrow J+2$	1	21	-0.52	96.8	122.9	2.8
	4	20	1.11	53.0	69.8	3.8
	8	19	-1.05	48.1	67.2	4.0
	12	18	1.91	34.1	29.3	1.8
	17	17	3.31	20.8	5.7	0.4
	18	17	-4.60	12.8	2.2	0.2
	22	16	4.89	12.8	2.0	0.03
	⋮					

dipolar case [$\int F(K)/K dK$] than in the quadrupolar case [$\int F(K)K dK$]. This is similar to the behavior of the resonance factors for dipole-dipole and quadrupole-quadrupole interactions derived by Van Kranendonk²⁶

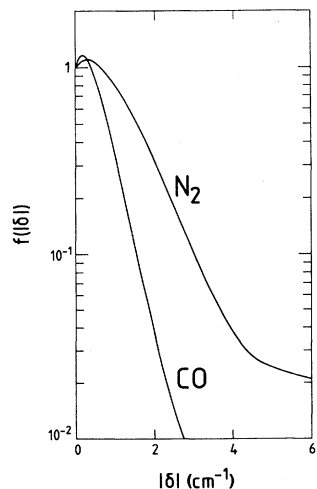


FIG. 4. The normalized resonance function for $Rb(nl)-N_2$ [$f(x) = e^{-0.9x}(1 + 1.76x - 0.87x^2 + 0.113x^3)$] and $Rb(nl)-CO$ [$f(x) = e^{-2.2x}(1 + 4.71x - 3.31x^2 + 0.733x^3)$] internal energy transfer versus the energy defect of the reaction δ (cm^{-1}).

who has studied the Raman line broadening due to anisotropic intermolecular forces. He has shown that resulting from the longer range of the dipolar interaction the resonance factor is about half as wide as for the quadrupolar interaction. According to these curves the n -changing cross sections have been only calculated for the transitions with $|\delta| < 6 \text{ cm}^{-1}$ and are reported in Tables II and III.

The ionization cross sections have been calculated following the theoretical treatment of Matsuzawa.¹⁸ This result is expressed through the following relation:

$$\sigma_i(n, J \rightarrow J-2) = \frac{8\pi}{15} \frac{Q^2}{V} \frac{J(J-1)}{(2J+1)(2J-1)} I_q(n, \epsilon_0), \quad (17)$$

where

$$I_q(n, \epsilon_0) = \int_0^\infty \frac{dF_n}{d\epsilon}(K, \epsilon_0) K^2 dK. \quad (18)$$

Noting that the binary-encounter theory and the momentum distribution of excited hydrogen atoms averaged by Fock²⁷ was shown to be a good approximation,²⁸ we have found that $I_q(n, \epsilon_0)$ and hence the ionization cross section can be expressed by the following simple analytic expression:

$$I_q(n, \epsilon_0) = \frac{1}{3n\pi\beta^2} \left[\frac{3(\beta-1)(\beta+1)^2}{\sqrt{\beta}} \left(\frac{\pi}{2} - \arctan \frac{1-\beta}{2\sqrt{\beta}} \right) + 6\beta^2 + 4\beta + 6 \right], \quad (19)$$

where $\epsilon_0 = E_J - E_{J-2} - 1/2n^2$ and $\beta = 2n^2\epsilon_0$. For $\epsilon_0 \simeq 0$ we have $I_q(n, 0) = 64/15\pi n$. To calculate the collisional ionization cross section of $\text{Rb}(nl)$ with N_2 we must multiply σ_i given by Eqs. (17) and (19) by the rotational distribution f_J and sum this product over J from J_0 (the first rotational level contributing to ionization) up to $J=40$ (where the rotational population is completely negligible). The results are tabulated in Tables II and III. We discuss in the Appendix the similarity between the bound-bound and the bound-free transition for all the studied levels.

Finally we can express the total quenching cross section by Eq. (1) (listed in Tables II and III) and compare them to the experimental values (Figs. 1 and 2). The overall agreement is quite good and shows that for the s levels located close to a hydrogenic level³ the l mixing is dominant over the quadrupole induced transitions. For the d levels which are more nonhydrogenic the l mixing is smaller than for the s levels and the contribution of the e^- -quadrupole interactions is more pronounced. The calculated and experimental quenching cross sections by N_2 do not exhibit noticeable oscillations. In contrast there exists some oscillations in the CO data (see especially the $35d-39d$ range) that are well reproduced by the calculations. This oscillatory behavior is attributed to the presence or absence of strongly resonant n -changing collisions. We can also see in Figs. 1 and 2 that the overall agreement is generally better for the case of CO than for the case of N_2 especially for the nd level. We may invoke the use of the elastic scattering length as scattering amplitude in Eq. (6) which yields some discrepancies between experimental and theoretical l -mixing cross sections¹⁷ that may reach a factor of 2. In contrast for the inelastic transitions the interaction potential between the Rydberg electron and the molecular dipole is well known yielding a good approximation for the scattering amplitude.

IV. CONCLUSION

While the $\text{Rb}(nl)$ ($n=23-46$, $l=0, 2$) quenching by CO is mainly governed by quasiresonant energy transfers induced by the molecular dipole (long-range interaction between the Rydberg electron and the molecule) yielding n -changing reactions, the $\text{Rb}(nl)$ depopulation by N_2 is much less efficient and leads mainly to the quasielastic process of angular momentum mixing (short-range interaction). We may conclude that the nitrogen target is rather similar to the rare-gas atom target; in contrast the dipole in the CO molecule (though small) changes drastically the collisional process where the inelastic processes are dominant. Finally, as already demonstrated in paper

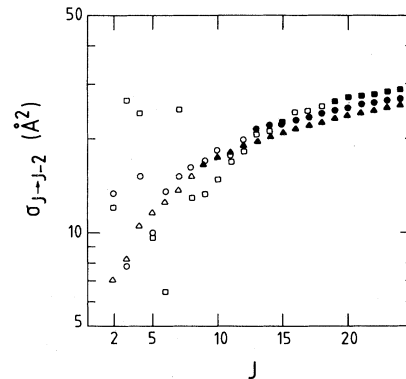


FIG. 5. $\sigma_{J \rightarrow J-2}$ is the cross section for the reaction $nl + \text{N}_2(J) \rightarrow \sum f + \text{N}_2(J-2)$, where $\sum f$ represents all the final atomic bound states or the continuum \square : 31s, \triangle : 46s, \circ : 35d. We adopt the following convention: $\square, \triangle, \circ$ represent bound-bound transitions when $\blacksquare, \blacktriangle, \bullet$ represent bound-free transitions.

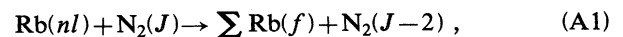
I, theoretical calculations based on the impulse approach are in good agreement with the experimental data.

ACKNOWLEDGMENT

We wish to thank Dr. B. Sayer for his critical reading of the manuscript.

APPENDIX

We can investigate the nl dependence of the cross section of the following reaction:



where $\sum \text{Rb}(f)$ represents all the final atomic bound or continuum states that significantly contribute to the $J \rightarrow J-2$ cross section. When we consider the scaling law [Eq. (15)] which gives the cross section of a particular transition, we can see that the $J \rightarrow J-2$ cross section is likely nl independent. If we say that for $|\delta| < |\delta_0|$ $f(\delta) = f(0)$ and for $|\delta| > |\delta_0|$ $f(\delta) \simeq 0$, the $J \rightarrow J-2$ cross section given by the summation over all final states is proportional to (\bar{n}'/n^2) for high enough n' values (\bar{n}' is the averaged quantum number of the final state) and as n and n' increase the ratios do not change drastically.

The nl independence of the $J \rightarrow J-2$ cross sections is clearly demonstrated with the help of Fig. 5. When the $J \rightarrow J-2$ rotational transition can populate more than 3-4 atomic levels there is no noticeable difference between two high Rydberg states. For example, for the 31s level for $J > 8$ the $J \rightarrow J-2$ cross section is quasiequal to the corresponding bound-bound or bound-free transition involving the 35d and 46s states. This indicates that the cross section for reaction (A1) only depends on the rotational energy lost by the molecule when $\bar{n}' > 40$.

- ¹L. Petitjean, F. Gounand, and P. R. Fournier, *Phys. Rev. A* **30**, 71 (1984).
- ²Different papers in *Rydberg States of Atoms and Molecules*, edited by R. F. Stebbings and F. B. Dunning (Cambridge University, Cambridge, 1982) are devoted to the thermal-energy collisions of Rydberg atoms with neutral particles.
- ³The quantum defect is $\delta_d = 1.35$ for the d states and $\delta_s = 3.13$ for the s states of Rb. Note that δ is used for the energy defect.
- ⁴M. Matsuzawa, *J. Chem. Phys.* **55**, 2685 (1971).
- ⁵T. F. Gallagher, R. E. Olson, W. E. Cooke, S. A. Edelstein, and R. M. Hill, *Phys. Rev. A* **16**, 441 (1977).
- ⁶T. F. Gallagher, S. A. Edelstein, and R. M. Hill, *Phys. Rev. Lett.* **35**, 644 (1975).
- ⁷T. F. Gallagher, S. A. Edelstein, and R. M. Hill, *Phys. Rev. A* **15**, 1945 (1977).
- ⁸C. Higgs, K. A. Smith, G. B. McMillian, F. B. Dunning, and R. F. Stebbings, *J. Phys. B* **14**, L285 (1981).
- ⁹F. B. Dunning and R. F. Stebbings, *Annu. Rev. Phys. Chem.* **33**, 173 (1982).
- ¹⁰T. F. Gallagher, W. E. Cooke, and S. A. Edelstein, *Phys. Rev. A* **17**, 125 (1978).
- ¹¹L. M. Humphrey, T. F. Gallagher, W. E. Cooke, and S. A. Edelstein, *Phys. Rev. A* **18**, 1383 (1978).
- ¹²T. F. Gallagher and W. E. Cooke, *Phys. Rev. A* **19**, 2161 (1979).
- ¹³M. Czajkowski, L. Krause, and G. M. Skardis, *J. Chem. Phys.* **51**, 1582 (1973).
- ¹⁴A. Hitachi, T. A. King, S. Kubota, and T. Doke, *Phys. Rev. A* **22**, 863 (1980).
- ¹⁵E. Bauer, E. R. Fisher, and F. R. Gilmore, *J. Chem. Phys.* **51**, 4173 (1969).
- ¹⁶R. Kachru, T. W. Mossberg, and S. R. Hartmann, *Phys. Rev. A* **22**, 1953 (1980).
- ¹⁷M. Hugon, B. Sayer, P. R. Fournier, and F. Gounand, *J. Phys. B* **15**, 2391 (1982).
- ¹⁸M. Matsuzawa, *J. Electron Spectrosc. Relat. Phenom.* **4**, 1 (1974).
- ¹⁹M. Matsuzawa, *J. Phys. B* **22**, 3743 (1979).
- ²⁰F. Gounand and L. Petitjean, *Phys. Rev. A* **30**, 61 (1984).
- ²¹E. de Prunelé and J. Pascale, *J. Phys. B* **12**, 2511 (1979).
- ²²E. Gerjuoy and S. Stein, *Phys. Rev.* **97**, 1671 (1955).
- ²³E. Gerjuoy and S. Stein, *Phys. Rev.* **98**, 1848 (1955).
- ²⁴A. Dalgarno and R. J. Moffett, *Proc. Natl. Acad. Sci. India Sect. A* **33**, 511 (1963).
- ²⁵O. H. Crawford, *J. Chem. Phys.* **47**, 1100 (1967).
- ²⁶J. Van Kranendonk, *Can. J. Phys.* **41**, 433 (1963).
- ²⁷V. Fock, *Z. Phys.* **98**, 145 (1935).
- ²⁸M. Matsuzawa, *Phys. Rev. A* **9**, 241 (1974).
- ²⁹K. P. Huber and G. Herzberg, in *Constants of Diatomic Molecules* (Van Nostrand, New York, 1979).
- ³⁰D. E. Strogryn and A. P. Strogryn, *Mol. Phys.* **11**, 371 (1966).